

A Phantom Design for Validating Colonoscopy Tracking

Jianfei Liu^a and Kalpathi R. Subramanian^b Terry S Yoo^c

^aImaging Biomarkers and Computer-Aided Diagnosis Laboratory,
Radiology and Imaging Sciences, Clinical Center,
National Institutes of Health, Bethesda, MD, 20892;

^bThe University of North Carolina at Charlotte
Charlotte Visualization Center, Dept. of Computer Science,
9201 University City Blvd, Charlotte, NC, 28223;

^cOffice of High Performance Computing and Communications,
National Library of Medicine, National Institutes of Health,
Bethesda, MD, 20892

ABSTRACT

Phantom experiments are useful and frequently used in validating algorithms or techniques in applications where it is difficult or impossible to generate accurate ground-truth. In this work we present a phantom design and experiments to validate our colonoscopy tracking algorithms, that serve to keep both virtual colonoscopy and optical colonoscopy images aligned (in location and orientation). We describe the construction of two phantoms, capable of respectively moving along a straight and a curved path. The phantoms are motorized so as to be able to move at a near constant speed. Experiments were performed at three speeds: 10, 15 and 20mm/sec, to simulate motion velocities during colonoscopy procedures. The average velocity error was within 3mm/sec in both straight and curved phantoms. Displacement error was within 7mm over a total distance of 288mm in the straight phantom, and less than 7mm over 287mm in the curved phantom. Multiple trials were performed of each experiment (and their errors averaged) to ensure repeatability.

Keywords: Colonoscopy Tracking, Optical Flow, Robust Regression, Egomotion Determination

1. INTRODUCTION

Well designed phantom experiments help generate accurate ground-truth, and are frequently used to validate the effectiveness and accuracy of algorithms and techniques used in clinical applications. This is especially the case in endoscopy applications where the ground truth is unknown and accuracy is evaluated by visual inspection or other qualitative means. Phantom experiments also allow experiments to be repeated under a set of controlled conditions, further improving the confidence in the underlying technique and across multiple trials.

In this work, we present design and evaluation of a straight and curved phantom for validating our colonoscopy tracking algorithms. The goal of tracking algorithms in endoscopy applications is the ability to simultaneously view aligned (location and orientation) pre-segmented virtual and optical endoscopy images¹⁻³ during the procedure (colonoscopy, bronchoscopy, etc.). Such technology can provide important clinical information to the gastroenterologist. Our research for the past several years has focused on tracking CT and optical colonoscopy image sequences,^{4,5} which is arguably a more challenging problem, as the colon can deform and has few topological or visual cues that can be exploited.

There are two approaches to validating endoscopy tracking algorithms. The first method employs virtual-to-virtual matching^{3,4} and a typical technique used in computer vision;⁶ virtual endoscopy image sequences are used as the testing datasets to perform virtual-to-virtual tracking validation. As camera motion parameters of

Further author information: (Send correspondence to Kalpathi R. Subramanian)

Jianfei Liu: E-mail: jianfei.liu@nih.gov

Kalpathi R. Subramanian: E-mail: krs@uncc.edu

Terry S Yoo: E-mail: yoo@nlm.nih.gov

every virtual image is known, the tracking error can be accurately measured. Such synthetic and ‘clean’ images are not a good fit, since factors such as fish-eye effects cannot be modeled or evaluated. Also, the navigation path followed in virtual images (along the centerline) is not realistic; navigation during a colonoscopy procedure can stretch the colon(telescoping), and turns in the (virtual) colon disappear. In order to resolve this issue, an alternate is to design physical phantoms, as used by a number of researchers.^{1,2,7,8} Magnetic sensors have also been used to collect endoscope motion parameters. The main disadvantage of this approach is repeatability; phantom experiments cannot be repeated under the same condition, resulting in decreased confidence in the experimental results.

The work presented here describes the design and application of a straight and curved phantom, for statistically testing our colonoscopy tracking algorithms. Experiments were repeatedly performed to test the accuracy of the algorithm, in terms of colonoscope’s velocity and displacement.

2. PHANTOM DESIGN

In designing the phantoms, we had the following requirements:

- Accurate measurement of camera motion parameters,
- Phantom should simulate a colon, i.e. a tunnel like shape is desirable,
- Sufficient visual cues (edges, corners) for optical flow computation,
- Repeatable experiments under the same conditions,
- Both curved and straight motion of the colonoscope, at speeds close to a real colonoscopy procedure.

Based on these requirements, we designed two colon phantoms, straight and curved, as seen in Fig. 1.

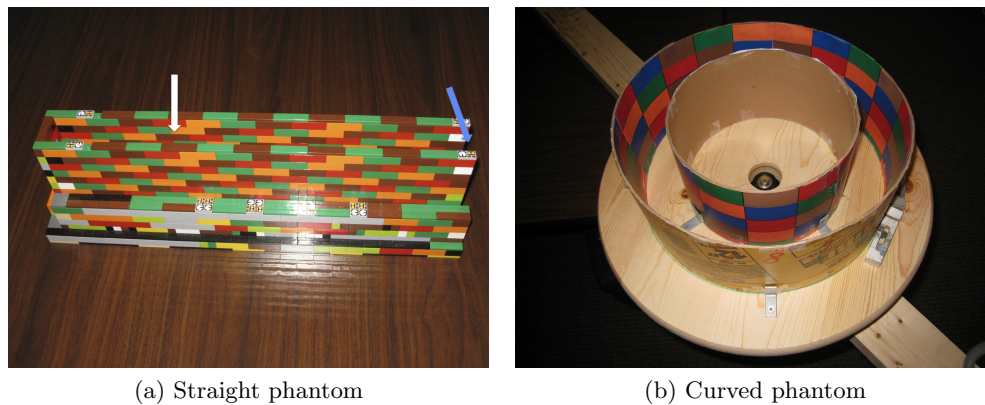
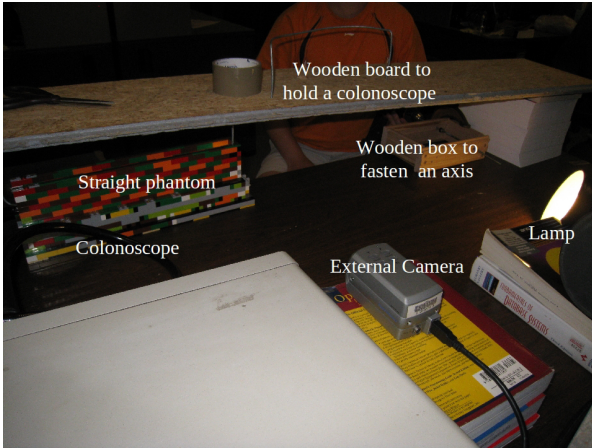


Figure 1: *Two types of colon phantoms.* (a) In the straight phantom, one end is left open, and used to insert the colonoscope(blue arrow). The top (white arrow) is uncovered, for observing the colonoscope’s movements, (b) In the curved phantom, the colonoscope is suspended between the inner and outer rings.

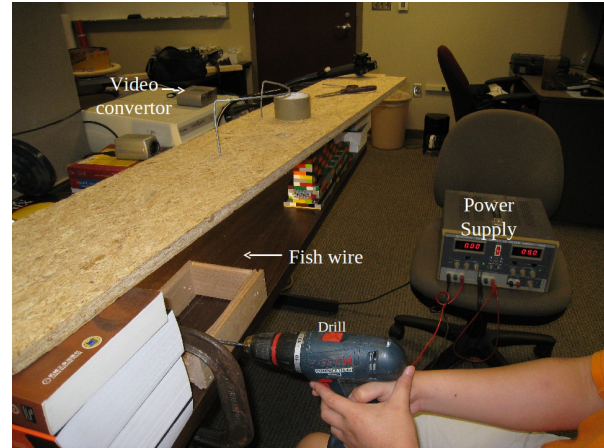
2.1. Straight Phantom Setup

LEGO bricks were used to build a straight-tunnel phantom (Fig. 1a) to take advantage of the many edges and corners for optical flow computation. LEGO bricks facilitate accurate measurement of the endoscope camera displacement, as it moves past each LEGO brick. The interior of the straight-tunnel phantom is 105mm×32mm×384mm.

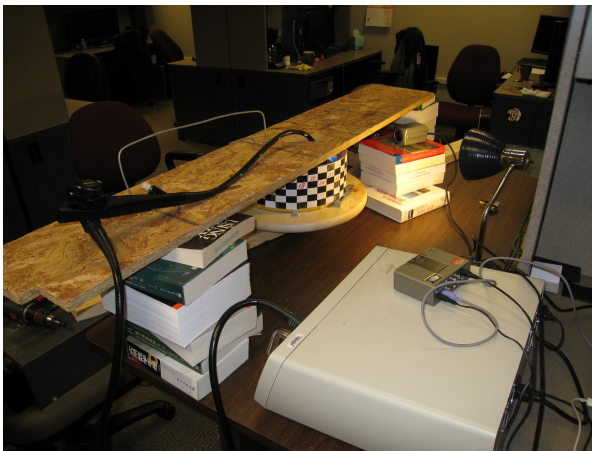
The straight phantom is driven by a motor, while the colonoscope remains stationary. Fig. 2a illustrates the straight phantom setup. A long wooden board is placed on top, and a straight iron wire is attached to the



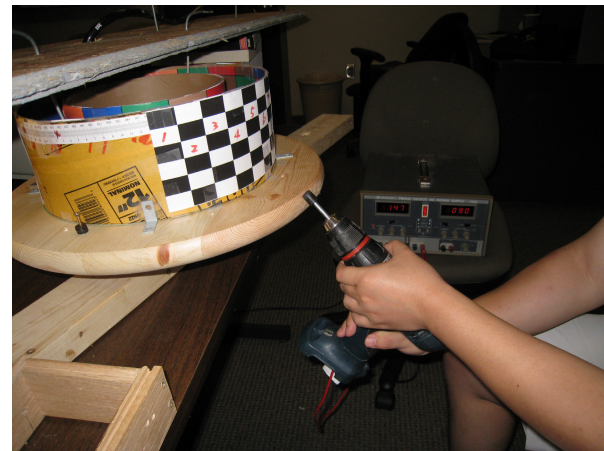
(a)



(b)



(c)



(d)

Figure 2: (a,b) The straight phantom experimental setup, (c,d) the curved phantom setup.

board to ‘suspend’ the colonoscope in the tunnel. The phantom is placed under the wooden board, with the colonoscope in the tunnel. A wooden box is fastened to a table by a clamp, and a steel rod is fixed inside this box, and one end of a fish wire is wound around the axis. The fish wire then passes through a small hole in the wooden box and the other end is connected to the straight phantom. An external video camera points to the straight phantom. A lamp is used to enhance the brightness. A drill controlled by a power supply rotates the axis at a constant speed, as shown in Fig. 2b. Finally, the images acquired by the external video camera and colonoscope are recorded.

2.2. Curved Phantom Setup

Two concentric sheets(thick cardboard) of radii 158.5mm and 102.5mm were used to build a curved phantom (Fig. 1b). The height of each sheet is 125mm. Textured (color squares) patterns coat the inside of the two curved sheets, generating visual cues for optical flow computation. The size of each colored square is 54mm×28mm.

Figs. 2c and Fig. 2d show the setup of the curved phantom. Instead of translating the curved phantom, a small wheel of radius 0.6mm is attached to the end of the drill, and used to rotate the turntable. Based on this speed reduction, the colonoscope can move at 10mm/sec while the drill can still rotate at high speeds.

2.3. Data Collection

In the straight phantom experiments, image sequences were collected at speeds of 10, 15, and 20mm/sec, which are typical speeds used during a colonoscopy procedure. Twenty-five trials were conducted at each speed. Of these, five sequences were selected, based on (1) the phantom's displacement divided by the total displacement time approximates the desired speed within 2mm/sec threshold, (2) each trial is approximately of the same total duration, within a tolerance of 0.3 sec. In all, fifteen exterior and interior straight phantom image sequences were collected at 10, 15, and 20mm/sec.

Similar to the straight phantom experiments, five exterior and five interior curved phantom image sequences were obtained at each of the three speeds.

3. EXPERIMENTAL RESULTS

Exterior phantom image sequences are used to determine the actual colonoscope motion, and interior image sequences are used to estimate the colonoscope's motion by the proposed tracking algorithm.⁴ Thus, the accuracy of the tracking algorithm can be analyzed by comparing the actual(ground truth) and estimated colonoscope motion.

3.1. Egomotion Estimation

Our egomotion estimation algorithm is described in detail in our earlier work.⁴ We begin by identifying a small set of accurate sparse optical flow vectors to measure the visual motion between successive colonoscopy images, and determine characteristic spatial-temporal scales for the current image. These spatial-temporal scales are used to accurately compute another visual motion representation, dense optical flow. Dense optical flow is employed to compute the focus of expansion (FOE), which is the intersection of camera translational direction and image plane; FOE computation permits separation of the computation of camera translational and rotational velocities, contributing to improved numerical robustness. The FOE and the sparse flow field are used to estimate the rotational velocity of the camera. Finally, the translational velocities are computed through elimination of the rotational components from the flow field.

3.2. Ground-truth Motion Determination

Parts of each sequence at the beginning and end were eliminated, representing acceleration and deceleration phases. In each sequence, we chose nineteen locations representing boundaries between LEGO bricks. The distance between consecutive bricks is 16mm. Assuming constant motor speed, the ground-truth velocities are determined by dividing the distance traveled (16mm) by the elapsed time. The ground-truth colonoscope displacements are then calculated by integrating ground-truth velocities.

Camera motion in the curved phantom is similarly measured; the outer walls are wrapped by a checkerboard pattern, with each square of size 29mm×19mm, as seen in Fig. 1b. The colonoscope's instantaneous speed is determined assuming that the colonoscope moves at a constant speed across the square. Finally, colonoscope displacements are determined by integrating ground-truth velocities.

3.3. Tracking Results

As described above, the ground-truth camera motion was determined from the exterior phantom images. The corresponding interior video streams are processed by our tracking algorithm. As the colonoscope camera has a strong fish-eye effect, acquired images are distorted. We analyzed the effect of this distortion on our tracking algorithm. The Matlab Toolbox⁹ was used to calibrate the camera and remove the distortion from the OC images. Note that straight edges between lego bricks in the straight phantom and colored squares in curved phantom become bent in the left column in Fig. 3. The right column images of Fig. 3 shows the same images after the distortion has been removed. The fish-eye effect can thus be understood by comparing the tracking results on the same colonoscopy image sequences, with and without camera calibration.

Fig. 4a and 5a shows the camera velocity plots on five phantom trials for the straight and curved phantoms at a speed of 10mm/sec; the upper and lower extents of these plots represent the maximum and minimum velocities across the five trials, while the solid curve in the middle represents the average velocity. The blue plot represents

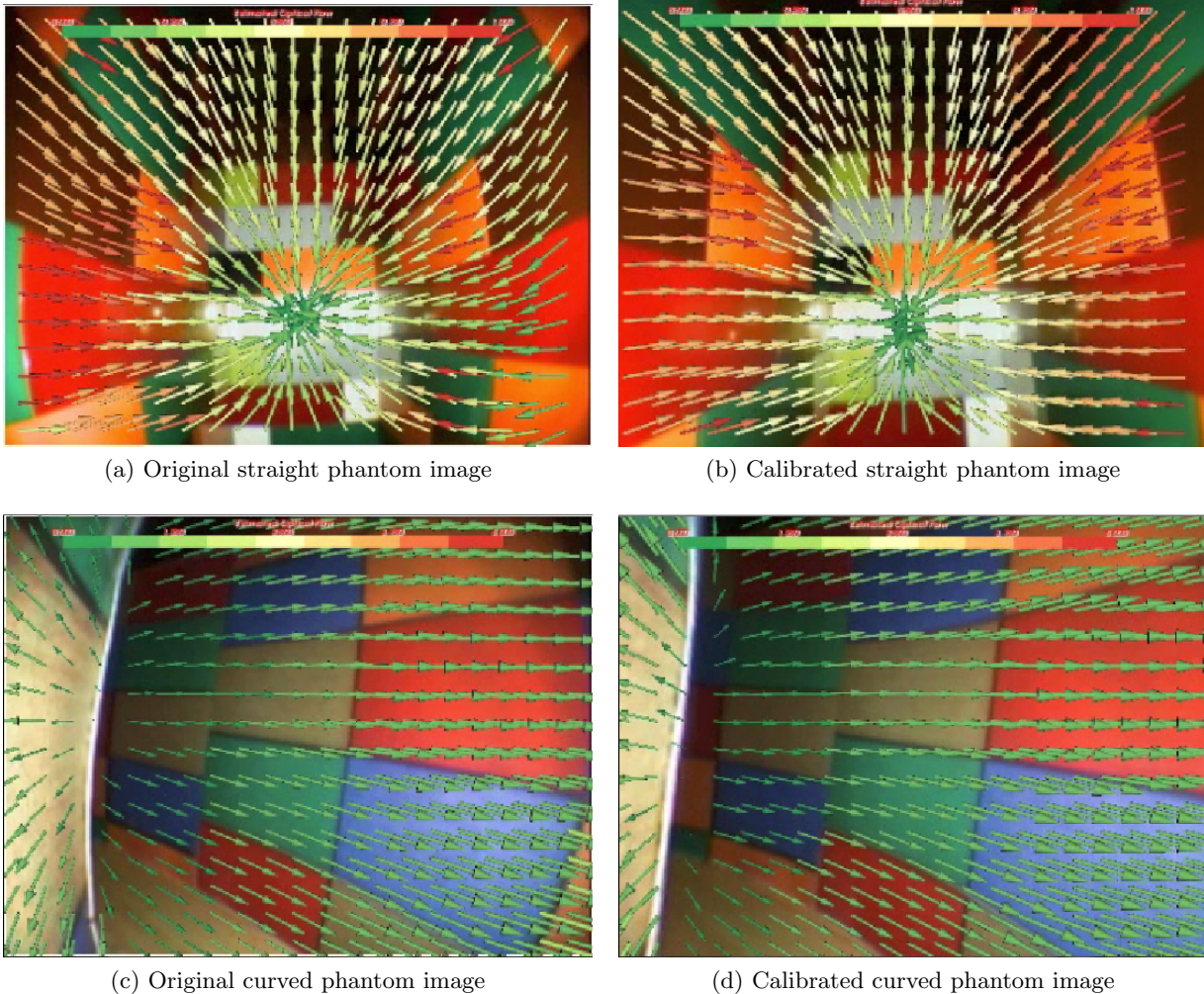
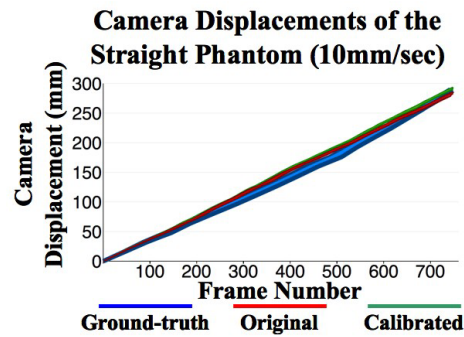
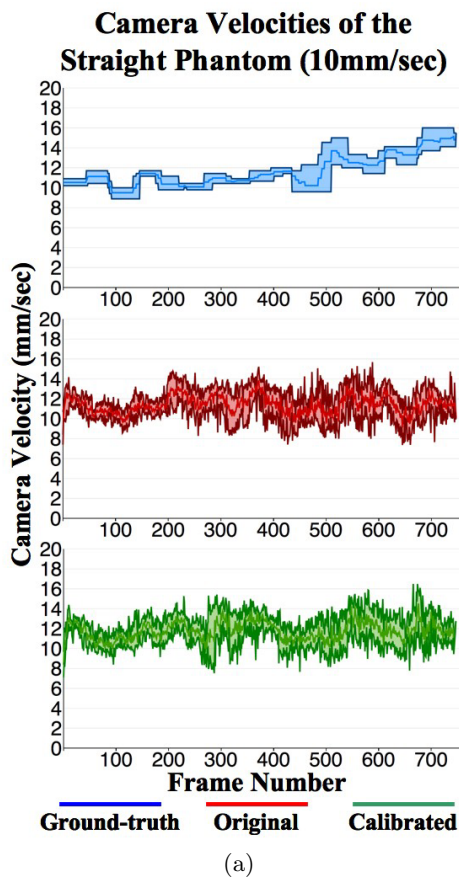


Figure 3: Original and calibrated images inside the straight (a, b) and curved phantoms (c,d).

the ground-truth velocities, while the red and green plots represent estimated camera velocity curves on the original and calibrated image sequences (five each). At 10mm/sec, average velocity error is less than 2mm/sec after tracking 750 images. The maximum velocity error is less than 8mm/sec on the original and calibrated phantom image sequences. Table 4c presents the average, maximum, and minimum estimated camera velocity errors of each of five trials. Fig. 4b shows the camera displacement plots. Average displacement error is less than 7mm across the five original phantom image sequences, and less than 9mm on the calibrated sequences. Maximum displacement error is less than 15mm on both original and calibrated image sequences. Table 4d gives the average, maximum, and minimum estimated camera displacement errors of each of five trials.

Fig. 5a shows the camera velocity curves on five curved phantom trials at a speed of 10mm/sec. Average velocity error is less than 2mm/sec on both original and calibrated phantom image sequences after tracking 750 images, and the maximum velocity error is less than 8mm/sec. Fig. 5b shows the corresponding camera displacement plots. Average displacement error is less than 2mm on the original phantom image sequences, and less than 4mm on the calibrated image sequences. Maximum displacement error is less than 5mm on the original image sequences and less than 10mm on the calibrated image sequences. Velocity and displacement results at speeds of 15mm/sec and 20mm/sec are consistent with those at 10mm/sec in both straight and curved phantoms. Table 5c presents the average, maximum, and minimum estimation errors of the camera velocity on original and calibrated phantom image sequences. Table 5d gives the average, maximum, and minimum estimation errors of



(b)

Img. Seq.	Original Images(mm/sec)			Calibr. Images(mm/sec)		
	Avg.	Max.	Min.	Avg.	Max.	Min.
1	1.68	6.36	0.004	1.66	5.93	0.01
2	1.52	5.23	0.005	1.6	5.05	0.002
3	1.97	7.2	0.01	1.99	7.4	0.0007
4	1.6	6.06	0.003	1.63	5.61	0.0006
5	1.64	6.11	0.003	1.53	5.81	0.003

(c) Errors in Camera velocity (Straight Phantom)

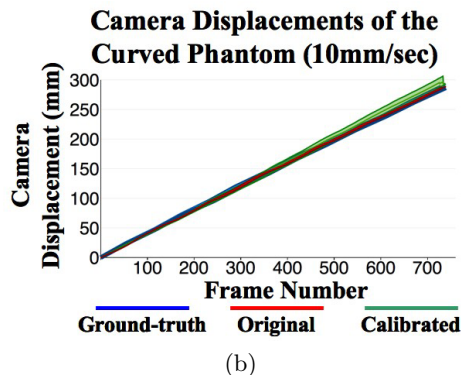
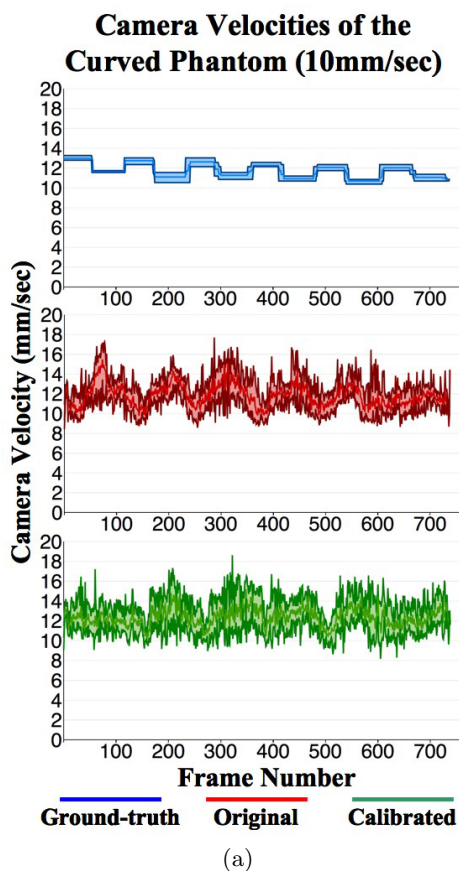
Img. Seq.	Original Images(mm)			Calibr. Images(mm)		
	Avg.	Max.	Min.	Avg.	Max.	Min.
1	5.92	11.89	0.0	8.7	12.33	0.0
2	4.26	8.72	0.0	7.46	9.87	0.0
3	6.55	10.44	0.0	8.58	11.91	0.0
4	6.5	12.19	0.0	8.4	13.3	0.0
5	6.87	14.65	0.0	8.21	14.57	0.0

(d) Errors in Camera displacement (Straight Phantom)

Figure 4: Velocity and displacement plots of the endoscope camera at 10mm/sec in the straight phantom. (a) camera velocity plots, (b) displacement plots. The blue plots represent the ground-truth camera velocities of five trials, and the red and green plots show the estimated velocities on the original and calibrated image sequences, respectively. The bottom and upper curves in each plot display the minimum and maximum velocities of the five trials, while the solid center curve represents the average velocities. The average velocity error is less than 2mm/sec on the original and calibrated phantom image sequences after 750 images have been tracked, and the maximum velocity error is less than 8mm/sec on both sequences. The average displacement error is less than 7mm on the original sequences, and it is less than 9mm on the calibrated sequences. The maximum displacement error of the five trials is less than 15mm on both sequences. Tables (c) and (d) detail the errors in camera velocities and displacements.

the camera displacements.

Similar results were obtained at speeds of 15mm/sec and 20mm/sec in the straight and curved phantom experiments. In the straight phantom, after 580 phantom images have been tracked at 15mm/sec, the average velocity error of five trials is less than 1.5mm/sec on both original and calibrated image sequences, and the maximum velocity error is less than 7mm/sec. The average displacement error is less than 3mm on the original phantom image sequence, and it is less than 5mm on the calibrated image sequences. The maximum displacement error of five trials is less than 6mm on the original image sequences and less than 8mm on the calibrated image sequences. At 20mm/sec, the average velocity error is less than 2mm/sec on both original and calibrated image sequences after 400 images have been tracked, and the maximum velocity error is less than 7mm/sec. The average displacement error is less than 2mm on the original phantom image sequences, and it is less than 4mm on the calibrated sequences. The maximum displacement error is less than 5mm on the original image sequences



Img. Seq.	Original Images(mm/sec)			Calibr. Images(mm/sec)		
	Avg.	Max.	Min.	Avg.	Max.	Min.
1	1.39	6.08	0.002	1.57	7.42	0.00
2	1.52	5.44	0.00	1.6	5.47	0.003
3	1.59	5.71	0.0015	1.31	5.43	0.002
4	1.49	5.69	0.0009	1.41	5.6	0.003
5	1.57	6.03	0.0004	1.56	6.62	0.004

(c) Errors in Camera velocity (Curved Phantom)

Img. Seq.	Original Images(mm)			Calibr. Images(mm)		
	Avg.	Max.	Min.	Avg.	Max.	Min.
1	1.3	3.86	0.0	2.82	7.45	0.0
2	0.99	3.27	0.0	1.23	9.8	0.0
3	1.32	4.22	0.0	2.84	6.18	0.0
4	1.64	3.85	0.0	3.76	10.2	0.0
5	1.29	3.8	0.0	1.94	4.44	0.0

(d) Errors in Camera displacement (Curved Phantom)

Figure 5: Velocity and displacement plots of the endoscope camera at 10mm/sec in the curved phantom. The average velocity error is less than 2mm/sec on the original and calibrated image sequences after 750 images have been tracked, and the maximum velocity error is less than 8mm/sec. The average displacement error is less than 2mm on the original sequences, and it is less than 4mm on the calibrated sequences. The maximum displacement error is less than 5mm on the original sequences and less than 10mm on the calibrated sequences. Tables (c) and (d) detail the errors in camera velocities and displacements.

and less than 7mm on the calibrated image sequences.

In the curved phantom, the average velocity error is less than 3mm/sec on both original and calibrated phantom image sequences after 550 images have been tracked at 15mm/sec. The maximum velocity error is less than 9mm/sec on the original image sequences, and it is less than 8mm/sec on calibrated image sequences. The average displacement error is less than 7mm on the original phantom image sequences, and it is less than 9mm on the calibrated sequences. The maximum displacement error is less than 10mm on the original image sequences and less than 13mm on the calibrated sequences. At 20mm/sec, the average velocity error is less than 3mm/sec on both original and calibrated image sequences after 470 images have been tracked. The maximum velocity error is less than 9mm/sec on the original image sequences and less than 8mm/sec on calibrated image sequences. The average displacement error is less than 6mm on the original phantom image sequences, and it is less than 7mm on the calibrated image sequences. The maximum displacement error is less than 9mm on the original image sequences and less than 10mm on the calibrated image sequences.

4. CONCLUSION

We can draw the following conclusions based on our phantom experiments:

1. In both straight and curved phantom experiments, the average estimated velocity error is less than 3mm/sec on the original and calibrated phantom image sequences at speeds of 10, 15 and 20mm/sec. Average displacement error is about 7mm over a total displacement of 287-288mm in the straight and curved phantoms. The colon is about 1500mm long and has six colon segments. Phantom experiments show that our tracking algorithm can accurately track the length of a full colon segment.
2. There is no significant difference in the camera velocity and displacement errors between the original and calibrated phantom image sequences, in both straight and curved phantom experiments. The estimated velocities from the calibrated phantom image sequences are slightly larger than those from the original sequences. The velocity increase arises because LEGO bricks in the straight phantom images or colored squares in the curved phantom images are artificially enlarged after the calibrated parameters are used to remove the image distortion, which increases the optical flow magnitudes. However, the tracking results are very comparable, as the average displacement error is less than 7mm in the original phantom image sequence and less than 9mm in the calibrated sequence.
3. Despite some variation of the ground-truth camera motion at the three speeds, the estimated camera velocity curves follow the same trend except that the velocity amplitudes are different. These results indicate that the estimated camera motion parameters rely on the actual camera motion as well as texture distributions inside the phantom. Periodic texture distributions can artificially influence the estimated camera velocities. Therefore, a random texture distribution could enhance estimation accuracy.
4. The number of tracked colonoscopy images dominates the errors in estimated camera displacements, while the actual speed of the colonoscope has a lesser effect. Camera displacement errors decrease with the increase of actual camera velocities because the slower the velocities, the greater the number of colonoscopy images.

REFERENCES

1. K. Mori, D. Deguchi, K. Ishitani, T. Kitasaka, Y. Suenaga, Y. Hasegawa, K. Imaizumi, and H. Takabatake, "Bronchoscope tracking without fiducial markers using ultra-tiny electromagnetic tracking system and its evaluation in different environments," in *Proc. of MICCAI*, pp. 644–651, 2007.
2. F. Deligianni, A. J. Chung, and G. Yang, "Non-rigid 2d-3d registration with catheter tip em tracking for patient specific bronchoscope simulation," in *Proc. of MICCAI*, pp. 281–288, 2006.
3. L. Rai, J. Helferty, and W. Higgins, "Combined video tracking and image-video registration for continuous bronchoscopic guidance," *International Journal of Computer Assisted Radiology and Surgery* **3**(3-4), pp. 315–329, 2008.
4. J. Liu, K. Subramanian, T. Yoo, and R. Uitert, "A stable optic-flow based method for tracking colonoscopy images," in *Proc. of Mathematical Methods in Biomedical Image Analysis*, pp. 1–8, 2008. June 27-28, Anchorage, Alaska.
5. J. Liu, K. Subramanian, and T. Yoo, "Region flow: A multi-stage method for colonoscopy tracking," in *Proc. of MICCAI*, 2010. September 20-24, Beijing, China.
6. O. M. Aodha, G. J. Brostow, and M. Pollefeys, "Segmenting video into classes of algorithm-suitability," in *Proceedings of IEEE Conference on Computer Vision and Pattern Recognition*, pp. 1054–1061, 2010.
7. K. Mori, D. Deguchi, K. Akiyama, T. Kitasaka, C. R. Maurer, Y. Suenaga, H. Takabatake, M. Mori, and H. Natori, "Hybrid bronchoscope tracking using a magnetic tracking sensor and image registration," in *Proc. of MICCAI*, **3750**, pp. 543–550, 2005.
8. J. Helferty, A. Sherbondy, A. Kiraly, and W. Higgins, "Computer-based system for the virtual-endoscopic guidance of bronchoscopy," *Computer Vision and Image Understanding* **108**, pp. 171–187, 2007.
9. J.-Y. Bouguet, "Camera calibration toolbox for matlab," 2010. www.vision.caltech.edu/bouguetj/calib_doc.